Journal of Solid State Chemistry **143,** 145–150 (1999)
Article ID jssc.1998.7939, available online at http://www.idealibrary.com on IDEAL®

# Synthesis and Structural Characterization of Two New Rare-Earth Manganese Germanates: $CeMn_2Ge_4O_{12}$ and $GdMnGe_2O_7$

C. Taviot-Guého,*,[1] P. Léone,† P. Palvadeau,† and J. Rouxel†

*Laboratoire des Matériaux Inorganiques, Université Blaise Pascal, 63177 Aubière Cedex, France; †Institut des Matériaux de Nantes, 2 rue de la Houssinière, 44322 Nantes Cedex 03, France

Received November 20, 1997; in revised form June 15, 1998; accepted June 24, 1998

**Crystals of $Ce^{+4}Mn_2^{+2}Ge_4O_{12}$ and $Gd^{+3}Mn^{+3}Ge_2O_7$ were obtained during the exploration of the quaternary Ln-Mn-Ge-O system. Their structures have been determined by single-crystal X-ray diffraction: $CeMn_2Ge_4O_{12}$ crystallizes in the tetragonal space group P4/nbm with $a = 9.816(1)$ Å, $c = 4.888(1)$ Å, $Z = 2$, and $R = 0.026$ while $GdMnGe_2O_7$ crystallizes in the orthorhombic space group A222 with $a = 4.735(1)$ Å, $b = 7.839(2)$ Å, $c = 13.500(3)$ Å, $Z = 4$, and $R = 0.048$. Both frameworks are built up from the same polyhedra, i.e., $LnO_8$ antiprisms, $MnO_6$ octahedra, and $GeO_4$ tetrahedra. $CeMn_2Ge_4O_{12}$ is isotypic with $SrNa_2P_4O_{12}$; the $GeO_4$ tetrahedra are linked into $Ge_4O_{12}$ rings located between layers of $CeO_8$ and $MnO_6$ polyhedra sharing edges. On the other hand, $GdMnGe_2O_7$ exhibits a novel quasi-one-dimensional lattice which might be ascribed to the Jahn–Teller nature of the $Mn^{+3}$ ion. The structure consists of chains of $MnO_6$ octahedra alternating with parallel chains of $GdO_8$ antiprisms forming layers linked together through $Ge_2O_7$ groups. A structural comparison with fluorite-related compounds as well as $CeMn_2Ge_4O_{12}$ will be discussed.** © 1999 Academic Press

## INTRODUCTION

The association of a transition metal element with a covalent element such as phosphorus, silicon, or germanium in oxides generates varied opened structures. Only a few of such compounds with manganese are reported in the literature although the peculiar behaviour of this element should make it possible to isolate a great number of new materials. Indeed, the coordination figures formed by oxygen atoms around manganese atoms are manifold and as a rule they exhibit four to eight ligands (1). Moreover, manganese can take various oxidation states ranging from II to VII. Finally, the Jahn–Teller nature of the $Mn^{3+}$ ($d^4$) ion might allow a unique framework to form.

Recently, our investigation of the system Ln-Mn-Si/Ge-O has produced interesting examples of oxo-compounds, $La_4Mn_5Si_4O_{22}$ (2) and $PrMnOGeO_4$ (3), containing rutile-like $MnO_2$ layers or infinite chains of $MnO_6$ octahedra, repectively. The quasi-low-dimensional character of these materials is enhanced by the presence of large rare-earth cations. Futhermore, $La_4Mn_5Si_4O_{22}$ displays the unusual characteristic of three oxidation states of manganese: $+2$, $+3$, and $+4$.

Over the years, the study of oxo-compounds characterized by quasi-one-dimensional chain or two-dimensional layer transition metal oxide structures which are isolated by closed-shell groups like silicate or phosphate anions, have recieved much attention. Besides the structural aspect, these compounds have shown to be of interest to the study of the behaviour of delocalized electrons in a confined lattice (4).

The present paper deals with the syntheses and the structural analyses of two new rare-earth manganese germanates: $Ce^{+4}Mn_2^{+2}Ge_4O_{12}$ and $Gd^{+3}Mn^{+3}Ge_2O_7$. $CeMn_2Ge_4O_{12}$ is isostructural with the anhydrous cyclotetraphosphate $SrNa_2P_4O_{12}$ (5), whereas $GdMnGe_2O_7$ exhibits a novel quasi-one-dimensional lattice formed by chains of $MnO_6$ octahedra which has not previously been observed in the large $AMX_2O_7$ compounds family (6, 7). A structural comparison with fluorite-related compounds (8) as well as $CeMn_2Ge_4O_{12}$ will be briefly discussed.

## EXPERIMENTAL SECTION

### *Synthesis and Characterization Techniques*

$CeMn_2Ge_4O_{12}$ and $GdMnGe_2O_7$ were prepared by a redox reaction involving $LnCl_3$ (Ln: Ce, Gd), $MnO_2$ and $GeO_2$:

$$2\ MnO_2 + 4\ GeO_2 + CeCl_3 \rightarrow CeMn_2Ge_4O_{12} + \tfrac{3}{2}\ Cl_2(g) \quad [1]$$

$$\tfrac{3}{2}\ MnO_2 + 2\ GeO_2 + GdCl_3 \rightarrow GdMnGe_2O_7 + \tfrac{1}{2}\ MnCl_2 + Cl_2(g). \quad [2]$$

[1] To whom the correspondence should be addressed. E-mail: gueho@chimtp.univ-bpclermont.fr.



0022-4596/99 $30.00
Copyright © 1999 by Academic Press
All rights of reproduction in any form reserved.

The reaction mixtures were placed in evacuated quartz tubes, then heated for 10 days at 700°C and slow-cooled at 10°C/h to room temperature. In order to avoid explosions due to chlorine gas emission, it is important to choose an adequate volume of the tube. The resulting product of reaction [2] was stirred in alcohol to dissolve the $MnCl_2$ matrix.

Both crystals of $CeMn_2Ge_4O_{12}$ and $GdMnGe_2O_7$ are light red needles.

The compositions were confirmed by X-ray microanalyses using a JEOL JSM-35C scanning electron microscope equipped with a Tracor TN 5500 micro Z system. $Mn_7SiO_{12}$ was a common impurity resulting from attack on the silica tube (9). Neither Si nor Cl impurity was detected in the crystals of $CeMn_2Ge_4O_{12}$ and $GdMnGe_2O_7$, however.

### *Structure Determination*

Initially, the single crystals used for data collection were investigated by oscillation and Weissenberg-type film methods. It is noteworthy that $GdMnGe_2O_7$ crystallizes in a noncentrosymmetric space group A222; attempts to refine the structure in the corresponding centrosymmetric space group Ammm (No. 65) failed. Data collection was performed on an Enraf-Nonius CAD4 diffractometer (see Table 1 for details). Both crystal structures were solved by direct and Fourier methods. They were refined by full-matrix least-squares techniques using the SHELXTL-PLUS program (10). Data were corrected for Lorentz polarization, absorption (11), and secondary extinction. The atomic scattering factors were those of Cromer and Waber (12) and the corrections for anomalous dispersions were from Cromer and Waber (13). Tables 2 and 4 list the final positional and thermal parameters.

**TABLE 1**
**Crystal Data, X-Ray Data Collection, and Structure Determination**

| | | |
|---|---|---|
| Empirical formula | $CeMn_2Ge_4O_{12}$ | $GdMnGe_2O_7$ |
| Formula weight (g/mol) | 732.42 | 469.40 |
| Crystal system | Tetragonal | Orthorhombic |
| Space group | P4/nbm (No. 125) | A222 (No. 21) |
| Lattice parameters: | | |
| a (Å) | 9.816(1) | 4.735(1) |
| b (Å) | 9.816(1) | 7.839(2) |
| c (Å) | 4.888(1) | 13.500(3) |
| V (Å$^3$) | 470.98 | 501.09 |
| Z | 2 | 4 |
| Temperature (K) | 294 | 294 |
| Color and habit | Light red needle | Light red needle |
| Crystal dimensions (mm) | $0.05 \times 0.03 \times 0.03$ | $0.05 \times 0.03 \times 0.03$ |
| $D_{calc}$ (g/cm$^3$) | 5.16 | 6.20 |
| Diffractometer | Enraf–Nonius CAD4 | Enraf–Nonius CAD4 |
| Radiation | MoK$\alpha$ ($\lambda = 0.71073$ Å) | MoK$\alpha$ ($\lambda = 0.71073$ Å) |
| $\mu_{(MoK\alpha)}$ (cm$^{-1}$) | 208.84 | 142.98 |
| Scan type | $\omega$ | $\omega$ |
| $\Theta$ range (°) | 1.0–50.0 | 1.5–50.0 |
| Scale factor | 1.86877 | 0.74322 |
| Quadrants measured ($hkl$) | $(-27, -1, -1)$ to $(27, 11, 9)$ | $(-27, 0, -1)$ to $(27, 11, 19)$ |
| No. of reflections measured | 1572 | 2226 |
| No. observations ($I > 3.00\sigma(I)$) | 404 | 1020 |
| No. variables | 27 | 54 |
| Corrections: Lorentz polarization Absorption | | |
| Residuals[a]: $R$, $R_w$ | 0.026, 0.028 | 0.048, 0.030 |
| Final diff. Fourier (e-/Å$^3$) | 1.94 | 3.90 |

[a] $R = \sum ||F_0| - |F_c|| / \sum |F_0|$ and $R_w = \sum (||F_0| - |F_c|| \cdot \sqrt{w}) / \sum (|F_0| \cdot \sqrt{w})$; $w = 1/\sigma^2(F_0)$.

## RESULTS AND DISCUSSION

### *$CeMn_2Ge_4O_{12}$*

The structure determination of $CeMn_2Ge_4O_{12}$ shows that it is isotypic with the anhydrous cyclotetraphosphate $SrNa_2P_4O_{12}$ (5). Compounds with the general formula $AB_2X_4O_{12}$ crystallize in three related structure types (5, 15): $M^I_2M^{II}P_4O_{12}$ ($M^I$ = K, $NH_4$, Rb, Tl and $M^{II}$ = Pb, Sr, Ba), $Na_2M^{II}P_4O_{12}$ ($M^{II}$ = Ca, Sr) and $Ca_2ZrSi_4O_{12}$. While many studies have been devoted to cyclophosphates and cyclosilicates, little data on the crystal structures of cyclogermanates have been reported (14).

The structure of $CeMn_2Ge_4O_{12}$ (Fig. 1) consists of (001) layers of $CeO_8$ antiprisms and distorted $MnO_6$ octahedra sharing edges (Fig. 2a), linked together via O-Ge-O bridges of the $Ge_4O_{12}$ rings; each $MnO_6$ octahedron shares all its corners with four different $Ge_4O_{12}$ rings (Fig. 2b).

Selected interatomic distances and bond angles are given in Table 3. The $Ge_4O_{12}$ rings show distances and angles similar to those found in other cyclotetragermanates (14(b)). The $MnO_6$ octahedra are elongated with two apical oxygen atoms at distances of 2.412 Å, longer than the four equatorial ones, 2.121 Å, leading to an averaged Mn-O distance of 2.218 Å expected for $Mn^{2+}$. This distorsion cannot be ascribed to Jahn–Teller effects for high spin $Mn^{2+}$ has a nondegenerate ground state. It may be noticed that sodium atoms in $SrNa_2P_4O_{12}$ exhibit a similar distorted octahedral coordination. Such distorted environments around $Mn^{2+}$ ions have already been observed in highly rigid frameworks of minerals (16). Bond valence sum calculations using Brese's tables (17) corroborate this oxidation state assignement; Mn gives 1.78 valence units (v.u.). Therefore, the oxidation state of cerium atoms must be 4+ in order to maintain the electroneutrality; the calculated valence is +3.58 v.u..

### *$GdMnGe_2O_7$*

$GdMnGe_2O_7$ exhibits a novel quasi-one-dimensional structure formed by chains of $MnO_6$ octahedra together

**TABLE 2**
**Positional and Equivalent Displacement Parameters for $CeMn_2Ge_4O_{12}$**

| Atom | Wyckoff | $x$ | $y$ | $z$ | $U_{eq}$ |
|---|---|---|---|---|---|
| Ce | 2b | 1/4 | 1/4 | 1/2 | 0.0053(1) |
| Mn | 4f | 0 | 0 | 1/2 | 0.0102(2) |
| Ge | 8k | 0.52379(6) | 1/4 | 0 | 0.0064(1) |
| O1 | 8m | − 0.3703(9) | 0.3703(9) | 0.1714(3) | 0.0086(9) |
| O2 | 16n | 0.1668(3) | 0.0643(4) | 0.2565(8) | 0.0081(8) |

with $Ge_2O_7$ groups and $GdO_8$ antiprisms. During the past years, a large number of compounds of stoichiometry $AMX_2O_7$ have been isolated (6, 7). Their mixed frameworks consist of $AO_m$ polyhedra (A: alkali or alkaline-earth metal; $m = 4$ to 10), $MO_n$ polyhedra ($M$: $M^{2+}$ or $M^{3+}$ transition metal; $n = 4$ to 6) and $X_2O_7$ groups ($X$: P, Si, Ge, As). Those built up from $MO_6$ octahedra incorporate either individual $MO_6$ octahedra or edge-sharing $M_2O_{10}$ bioctahedral units.To the best of our knowledge, none of them displays chains of $MnO_6$ octahedra.

Figure 3 shows the structure of $GdMnGe_2O_7$ viewed along the chains of corner-sharing $MnO_6$ octahedra. These undulating chains alternate with chains of edge-sharing $GdO_8$ antiprisms forming layers parallel to (100) (Fig. 4a). In the a direction, the $MnO_6$ chains are cross-linked via O-Ge-O bridges of the $Ge_2O_7$ groups resulting other layers that can be described as containing $MnGe_2O_{11}$ units (Fig. 4b). Each unit, in which one $Ge_2O_7$ group shares two of its apices with the same $MnO_6$ octahedron, is linked to

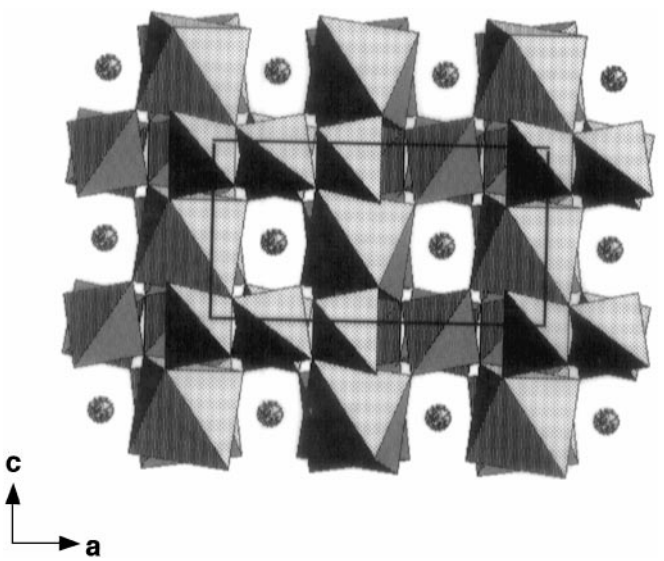


**FIG. 1.** Structure of $CeMn_2Ge_4O_{12}$ in the *ac*-plane. Small filled circles represent cerium atoms.

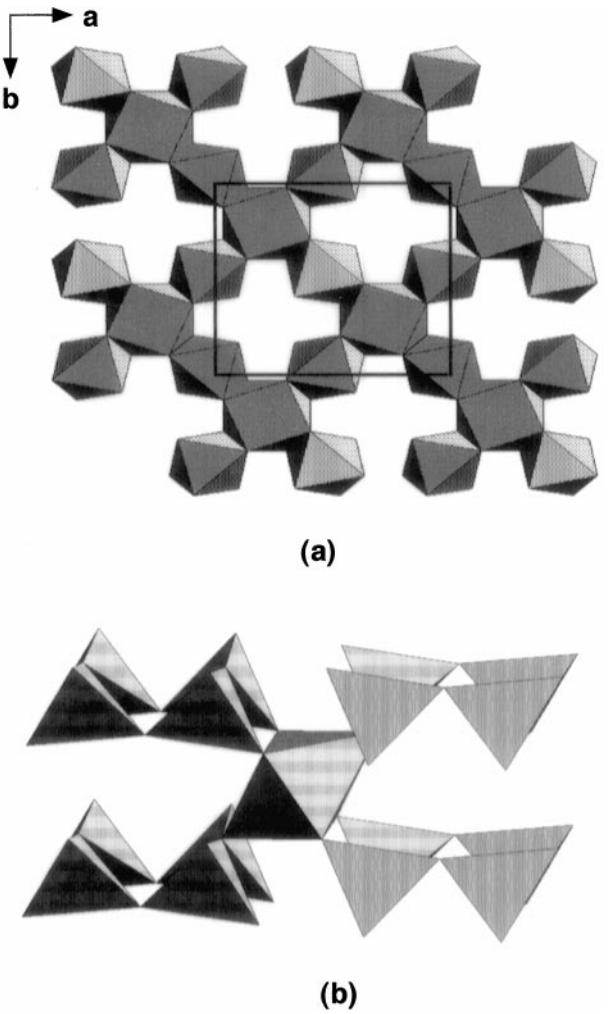


**FIG. 2.** (a) (001) layers in $CeMn_2Ge_4O_{12}$ formed by $MnO_6$ octahedra and $CeO_8$ antiprisms sharing edges; (b) these layers are connected in the $c$ direction by $Ge_4O_{12}$ rings.

five other units lying in the same plane. Such an arrangement of $MO_6$ and $X_2O_7$ polyhedra has never been shown so far. On the other hand, $GdMnGe_2O_7$ possesses the same arrangement of $MO_6$-$LnO_8$ slabs as in the fluorite-related phases $Ln_3MO_7$ (Ln: rare-earth, Y or Sc and $M$: Nb, Sb, or Ta) (8), as well as in the pyrochlore and weberite compounds (18). They differ basically only in the interslab cations though the $LnO_8$ polyhedra are nearly cubes in the latter compounds.

Table 5 lists selected bond lengths and angles for $GdO_8$, $MnO_6$, and $Ge_2O_7$ polyhedra. Bond valence sum calculations for Mn and Ge sites are consistent with their formal oxidation states at $+2.99$ and $+3.81$ v.u., respectively. The distorted octahedral coordination of the Mn site with Mn-O axial bond lengths of 2.464 Å much longer than the equatorial ones, 1.932–1.883 Å, is suitable to the Jahn–Teller nature of the $Mn^{3+}$ ion. The $MnO_6$ octahedra are linked

**TABLE 3**
**Important Bond Lengths (Å) and Angles (°) in $CeMn_2Ge_4O_{12}$**

| | | | | | | |
|---|---|---|---|---|---|---|
| Ce | O2 × 8 | 2.325(4) | | | | |
| Mn | O1 × 2 | 2.412(4) | O1 | Mn | O1 | 180.0 |
| | O2 × 4 | 2.121(4) | O2 | Mn | O2 | 180.0 × 2 |
| | | | | | | 81.7(2) × 2 |
| | | | | | | 98.3(2) × 2 |
| | | | O1 | Mn | O2 | 97.1(2) × 4 |
| | | | | | | 82.9(2) × 4 |
| Ge | O1 × 2 | 1.783(6) | O1 | Ge | O1 | 108.7(1) |
| | O2 × 2 | 1.728(4) | O2 | Ge | O2 | 120.0(2) |
| | | | O1 | Ge | O2 | 105.3(2) × 2 |
| | | | | | | 108.6(2) × 2 |
| | | | Ge | O1 | Ge | 123.5(3) |

through the mutual sharing of the oxygen atom O1. It is worth pointing out the high coordination number of this oxygen atom which is both the bridging oxygen atom of $MnO_6$ chains and $Ge_2O_7$ groups. Bond valence sum calculations show a weak contribution of the long Mn-O1 bonds, $\upsilon_{Mn-O1} = +0.15$ v.u., allowing O1 to be shared with the $Ge_2O_7$ groups, $\upsilon_{Ge-O1} = +0.86$ v.u. The sum is in good agreement with the formal oxidation state of oxygen anion: $-2.02$ v.u. The zigzag configuration of $MnO_6$ chains is also rather uncommon: the long Mn-O1 bond results in a long Mn—Mn separation distance, 3.921 Å, with a very bent Mn-O1-Mn bond angle 105.5°. From these observations, it is inferred that only the Jahn–Teller nature of the $Mn^{3+}$ cation would make it possible for such a constrained framework to be stabilized.

The environment of the rare-earth cation is an antiprism $GdO_8$ with Gd-O bond lengths ranging from 2.341 Å to 2.428 Å. The calculated valences are $+3.49$ for Gd1 and $+3.39$ for Gd2. The $GeO_4$ tetrahedra forming the $Ge_2O_7$ groups are distorted with Ge-O distances varying from 1.724 Å to 1.804 Å and O-Ge-O bond angles from 99.4 to 120.3°; this is due to the complex bond interaction occuring at each oxygen anion.

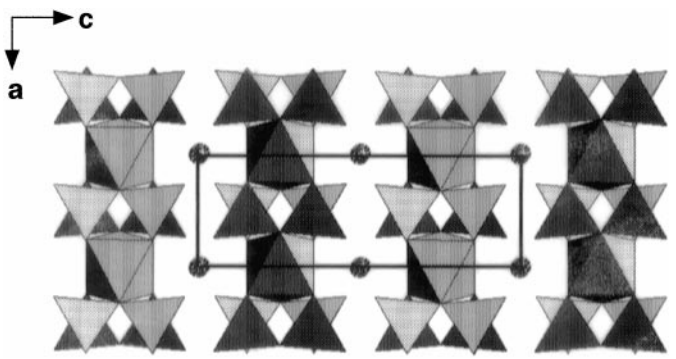


**FIG. 3.** Structure of $GdMnGe_2O_7$ in the *ac*-plane. Small filled circles represent gadolinium atoms.

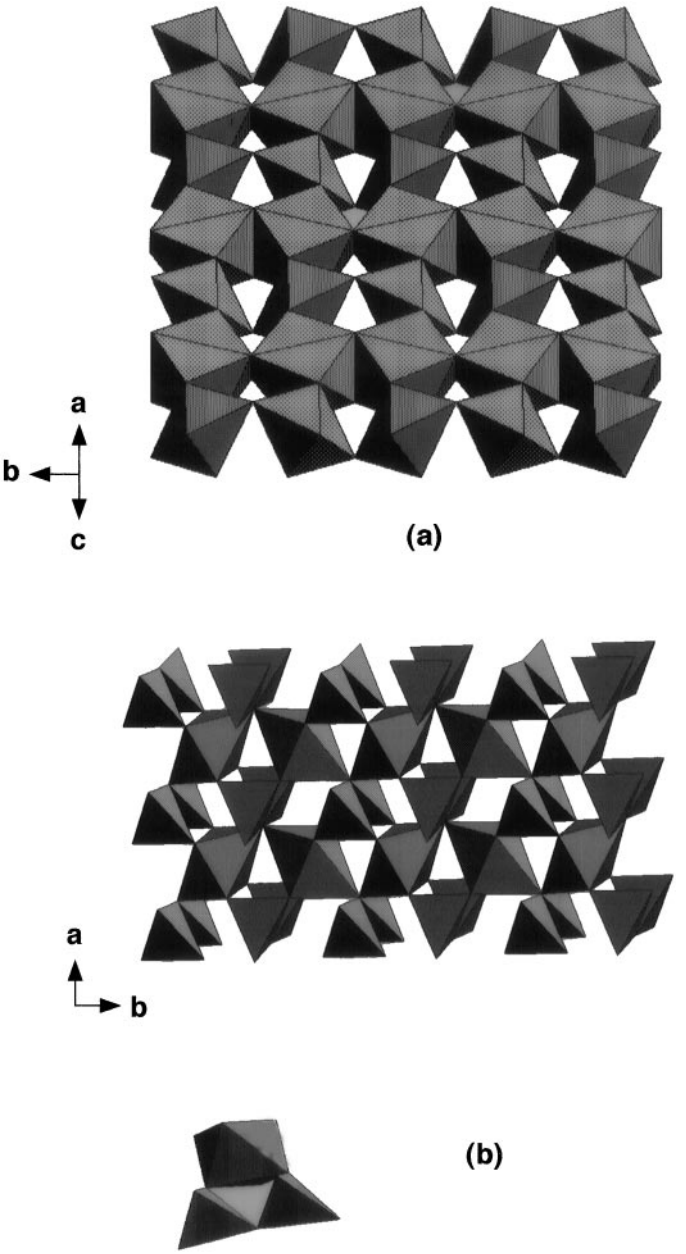


**FIG. 4.** (a) (100) layers in $GdMnGe_2O_7$ formed by alternating chains of $MnO_6$ octahedra and $GdO_8$ antiprisms. (b) The chains of $MnO_6$ octahedra are linked in the *a* direction through $Ge_2O_7$ groups resulting other layers parallel to (001) that can be described as containing $MnGe_2O_{11}$ units.

An interesting structural correlation can be drawn between $GdMnGe_2O_7$ and $CeMn_2Ge_4O_{12}$. Both structures are built up from the same polyhedra and the chemical formula of $GdMnGe_2O_7$ can be rewritten $Gd_2Mn_2Ge_4O_{14}$. Then, the two compounds differ from each other by two oxygen anions and a rare-earth cation whose charges are balanced by different electropositive cations, $Ce^{4+}$ versus

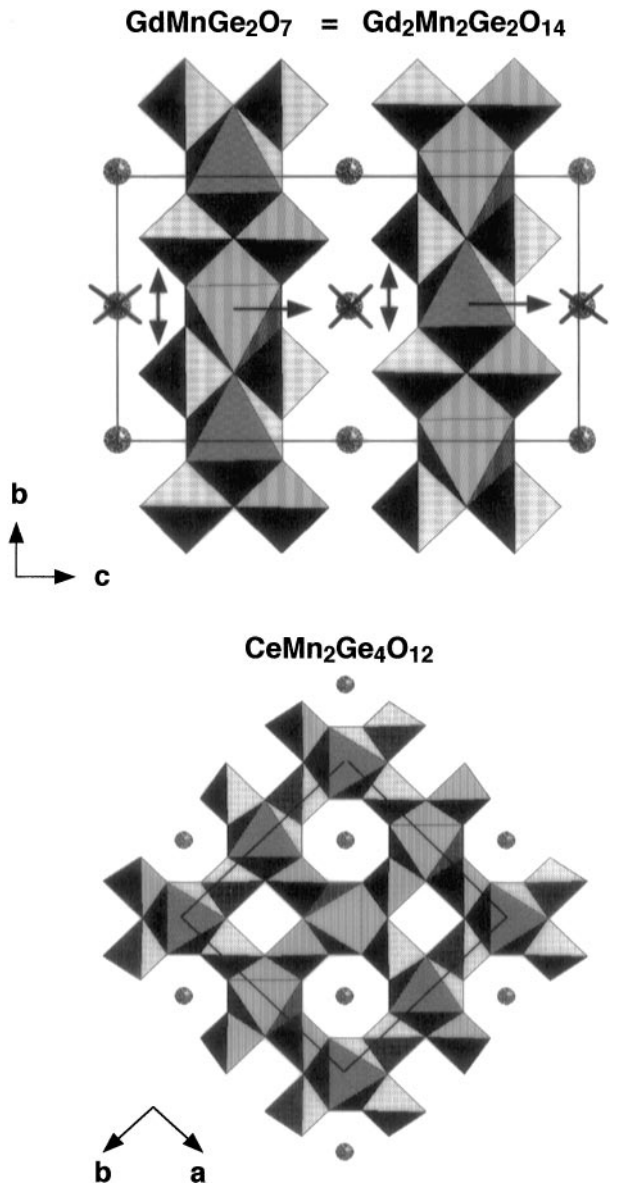


**FIG. 5.** Structural relationship between $GdMnGe_2O_7$ and $CeMn_2Ge_4O_{12}$. Filled circles marked with a cross represent rare-earth atoms in $GdMnGe_2O_7$ that are replaced by Mn atoms in $CeMn_2Ge_4O_{12}$.

**TABLE 4**
**Positional and Equivalent Displacement Parameters for $GdMnGe_2O_7$**

| Atom | Wyckoff | $x$ | $y$ | $z$ | $U_{eq}$ |
|---|---|---|---|---|---|
| Gd1 | 2a | 0 | 0 | 0 | 0.0029(3) |
| Gd2 | 2b | 0 | 1/2 | 0 | 0.0071(4) |
| Mn | 4e | 0 | 0 | 0.7536(3) | 0.0050(2) |
| Ge | 8l | − 0.5186(2) | − 0.2488(4) | − 0.13708(4) | 0.0053(3) |
| O1 | 4k | − 0.3151(9) | − 3/4 | − 3/4 | 0.007(1) |
| O2 | 8l | 0.238(2) | − 0.425(1) | − 0.1457(8) | 0.008(1) |
| O3 | 8l | − 0.2626(7) | 0.246(2) | 0.0462(3) | 0.008(1) |
| O4 | 8l | 0.244(1) | 0.080(1) | 0.1466(8) | 0.005(1) |

**TABLE 5**
**Important Bond Lengths (Å) and Angles (°) in $GdMnGe_2O_7$**

| | | | | | | |
|---|---|---|---|---|---|---|
| Gd1 | O3 × 4 | 2.379(14) | | | | |
| | O4 × 4 | 2.377(10) | | | | |
| Gd2 | O2 × 4 | 2.341(10) | | | | |
| | O3 × 4 | 2.428(15) | | | | |
| Mn | O1 × 2 | 2.464(3) | O1 | Mn | O1 | 177.7(2) |
| | O2 × 2 | 1.932(10) | | | O2 | 82.8(3) × 2 |
| | O4 × 2 | 1.883(10) | | | O2 | 95.5(3) × 2 |
| | Mn × 2 | 3.921(4) | | | O4 | 96.8(3) |
| | | | | | O4 | 96.9(3) |
| | | | | | O4 | 84.8(3) × 2 |
| | | | O2 | Mn | O2 | 82.1(6) |
| | | | | | O4 | 176.7(5) × 2 |
| | | | | | O4 | 94.6(4) × 2 |
| | | | O4 | Mn | O4 | 88.6(6) |
| | | | Mn | O1 | Mn | 105.5(2) |
| Ge | O1 | 1.803(3) | O1 | Ge | O2 | 106.5(3) |
| | O2 | 1.804(11) | | | O3 | 103.1(2) |
| | O3 | 1.724(4) | | | O4 | 106.6(4) |
| | O4 | 1.740(11) | O2 | Ge | O3 | 120.3(6) |
| | | | | | O4 | 99.4(5) |
| | | | O3 | Ge | O4 | 119.9(6) |
| | | | Ge | O1 | Ge | 115.4(3) |

$Gd^{3+}$ and $Mn^{2+}$ versus $Mn^{3+}$. As can be seen in Fig. 5, one could imagine the change from $Gd_2Mn_2Ge_4O_{14}$ to $CeMn_2Ge_4O_{12}$ in three steps: first, half the rare-earth sites are removed, then, half the $MnO_6$ octahedra are placed on these free sites, and finally, the $Ge_2O_7$ pairs facing each other are fused to give $Ge_4O_{12}$ cycles.

## REFERENCES


1. E. F. Bertaut, G. Buisson, A. Durif, J. Mareschal, M. C. Montmory, and S. Quezel-Ambrunaz, *Colloq. Int. CNRS Soc. Chim.* **5,** 1132 (1965).
2. C. Gueho, D. Giaquinta, J. L. Mansot, T. Ebel, and P. Palvadeau, *Chem. Mater.* **7,** 486 (1995).
3. C. Gueho, D. Giaquinta, P. Palvadeau, and J. Rouxel, *J. Solid State Chem.* **7,** 120 (1995).

4a. J. Rouxel, "Crystal Chemistry and Properties of Materials with Quasi-One -Dimensional Structures," Vol. 291, p. 263. Reidel, Dordrecht, 1986.

4b. R. C. Hausalter, M. E. Wang, J. Thompson, J. Zubieta, and C. J. O'Connor, *J. Solid State Chem.* **109,** 259 (1994).

4c. S. Wang and S. J. Hwu, *J. Am. Chem. Soc.* **114,** 6920 (1992).

4d. S. Wang, S.-J. Hwu, J. A. Paradis, and J. Whangbo, *J. Am. Chem. Soc.* **117,** 5515 (1995).

5. M. T. Averbuch-Pouchot and A. Durif, *Acta Crystallogr. Sect. C* **39,** 811 (1983).

6a. E. Dvoncova and K. H. Lii, *J. Solid State Chem.* **105,** 279 (1993).

6b. L. Benhamada, A. Grandin, M. M. Borel, A. Leclaire, and B. Raveau, *Acta Crystallogr. Sect. C* **47,** 424 (1991).

6c. K. H. Lii, Y. P. Wang, Y. B. Chen, and S. L. Wang, *J. Solid State Chem.* **86,** 143 (1990).

6d. S. L. Wang, P. C. Wang, and Y. P. Nieh, *J. Appl. Crystallogr.* **23**, 520 (1990).
6e. Y. P. Wang, K. H. Lii, and S. L. Wang, *Acta Crystallogr. Sect. C* **45,** 673 (1989).
6f. Y. P Wang and K. H. Lii, *Acta Crystallogr Sect. C* **45,** 1210 (1989).
6g. D. Riou, A. Leclaire, A. Grandin, and B. Raveau, *Acta Crystallogr. Sect. C* **45,** 989 (1989).
6h. J. J. Chen, C. C. Wang, and K. H. Lii, *Acta Crystallogr. Sect. C* **45,** 673 (1989).
6i. A. Leclaire, M. M. Borel, A. Grandin, and B. Raveau, *J. Solid State Chem.* **78,** 220 (1989).
7a. R. D. Adams, R. Layland, and C. Payen, *Polyhedron*, **23–24,** 3473 (1995).
7b. D. Riou and B. Raveau, *Acta Cryst. C* **47,** 1708 (1991).
7c. A. Moqine, A. Boukhari, and E. M. Holt, *Acta Cryst. C* **47,** 2294 (1991).
7d. D. Riou, H. Leligny, C. Pham, P. Labbe, and B. Raveau, *Acta Cryst. B* **47,** 608 (1991).
7e. D. Riou and M. Goreaud, *Acta Cryst. C* **46,** 1191 (1990).
8. H. J. Rossel, *J. Solid State Chem.* **27,** 115 (1979).
9. P. Euzen, M. Queignec, P. Palvadeau, J. P. Venien, *Mat. Res. Bull.* **26,** 841 (1991).
10. *SHELXTL PLUS 4.0*, Siemens Analytical X-Ray Instruments, Madison, WI, 1989.
11. A. C. North, D. C. Phillips, and F. S. Matthews, *Acta Crystallogr. A* **24,** 351 (1968).
12. D. T. Cromer and J. T. Waber, *in* "International Tables for X-Ray Crystallography," Vol. 2.2A. Kynoch, Birmingham, UK, 1974.
13. D. T. Cromer and J. T. Waber, *in* "International Tables for X-Ray Crystallography," Vol. 2.3.1. Kynoch, Birmingham, UK, 1974.
14a. K. K. Palkina, S. I. Maksimova, V. G. Kuznetsov, and N. N. Chudinova, *Sov. Phys. Dokl* **24,** 243 (1979).
14b. C. Pagnoux, A. Verbaere, Y. Kanno, Y. Piffard, and M. Tournoux, *J. Solid State Chem.* **99,** 173 (1992).
14c. A. Y. Barkov, Y. P. Men'Shikov, V. D. Begizov, and A. I. Lednev, *Eur. J. Mineral.* **8,** 311 (1996).
15a. C. Cavero-Ghersi and A. Durif, *J. Appl. Cryst.* **8,** 562 (1975).
15b. S. Colin, B. Dupre, G. Venturini, B. Malaman, and C. Gleitzer, *J. Solid State Chem.* **102,** 242 (1993).
15c. M. T. Averbuch-Pouchot, *Eur. J. Solid State Inorg. Chem.* **33,** 15 (1996).
16. P. B. Moore and T. Araki, *Am. Mineral.* **64,** 390 (1979).
17. N. E. Brese and M. O'Keeffe, *Acta Cryst. B* **47,** 192 (1991).
18a. A. Byström, *Ark. Kem. Min. Geol. A* **18**(10), (1944).
18b. A. Byström, *Ark. Kem. Min. Geol. A* **18**(21), (1944).